

Brief Reports

Brief Reports are accounts of completed research which, while meeting the usual Physical Review standards of scientific quality, do not warrant regular articles. A Brief Report may be no longer than four printed pages and must be accompanied by an abstract. The same publication schedule as for regular articles is followed, and page proofs are sent to authors.

Internal strain effects on the phase diagram of Ni-Pt alloys

C. Amador

*Department of Physics, Case Western Reserve University, Cleveland, Ohio 44106-7079
and Facultad de Química, Universidad Nacional Autónoma de México,
Ciudad Universitaria, 04510 Distrito Federal, México**

W. R. L. Lambrecht

Department of Physics, Case Western Reserve University, Cleveland, Ohio 44106-7079

M. van Schilfgaarde

SRI International, 333 Ravenswood, Menlo Park, California 94025

B. Segall

Department of Physics, Case Western Reserve University, Cleveland, Ohio 44106-7079

(Received 23 February 1993)

An effective-cluster-volume approximation is introduced to describe the average effect of bond-length relaxations in an alloy with large size mismatch, e.g., Ni-Pt. It is shown that this approach leads to good agreement with the experimental critical temperatures and with the measured energy of formation of disordered alloys.

Much progress has been made in understanding the origin of alloy phase diagrams using generalized Ising spin models. To complete this understanding, however, it is important to determine the Ising interaction parameters in terms of the underlying electronic structure. Several routes for achieving this have been proposed, among which is the Connolly-Williams (CW) approach.¹ It has the significant advantage of most readily allowing for the inclusion of one of the most accurate means of obtaining the solid's total energy, local-density-functional theory.² Alternative alloy theories and their relative merits are discussed, e.g., in Ref. 3. Our purpose is to show that the correct energy and hence temperature scale of the phase diagram of an alloy with large size mismatch between the constituents can be obtained using a slight generalization of the CW approach. The generalization consists in the proper inclusion of internal strain of the individual bond lengths through the introduction of an "effective cluster volume." The inclusion of internal strain clearly should be important in other alloy approaches as well.

The CW approach is based on mapping of the energy of formation of the alloy to a generalized Ising spin Hamiltonian,⁴

$$\begin{aligned} \Delta E_{\sigma}(V) &= E_{\sigma}(V) - (1-x)E_A(V_A) - xE_B(V_B), \\ &= \sum_i \xi_{\sigma i} J_i(V), \end{aligned} \quad (1)$$

using (in general, volume-dependent) effective interaction parameters $J_i(V)$ and correlation functions $\xi_{\sigma i}$. The total energies of pure A and B solids and an arbitrary alloy configuration σ of composition $A_{1-x}B_x$ at volume V are

denoted E_A , E_B , and E_{σ} , respectively. The CW approach consists in applying Eq. (1) to a set of ordered configurations, whose energies can be calculated from first principles, and inverting the equation to extract the $J_i(V)$. One thus obtains

$$\Delta E_{\sigma}(V) = \sum_n P_{\sigma n} \Delta E_n(V), \quad (2)$$

where $\Delta E_n(V)$ are the energies of formation as a function of volume of the reference configurations n with the coefficients $P_{\sigma n} = \sum_i \xi_{\sigma i} [\xi^{-1}]_{in}$.

If, for fcc-derived alloys, one truncates the cluster expansion (1) at the nearest-neighbor tetrahedron and selects the CW structures (fcc for A and B , $L1_2$ for A_3B and AB_3 , and $L1_0$ for A_2B_2), the $\Delta E_n(V)$ in Eq. (2) acquire the simple meaning of being the energy contributions of the corresponding $A_{4-n}B_n$ tetrahedra. Correspondingly, the $P_{\sigma n}$ become the probabilities of the occurrence of these clusters in the configuration σ . For simplicity, we adopt this physically transparent form of the theory.

For Ni-Pt the above-defined tetrahedron approximation appears at first sight to be sufficient since a successful fit of the phase diagram⁵ with adjustable (volume-independent) interaction parameters was obtained by Dahmani *et al.*⁶ On the other hand, the large size mismatch in the Ni-Pt system is expected to lead to important lattice relaxations. Since the latter may lead to long-range interactions,⁷⁻⁹ the tetrahedron approximation might seem insufficient. Previous electronic structure studies of Ni-Pt focused on relativistic effects on the

sign of the formation energies^{10,11} and the incipient tendency to $L1_0$ ordering in the disordered phase,¹² but not on the phase diagram.

To make the importance of the internal strain clear, we first consider the results obtained using the conventional CW approach in Table I. The first approach we consider is to use *volume-independent* (VI) cluster energies taken to be the energies of formation of the CW structures each at their own equilibrium volume, i.e., $\Delta E_n(V_n^{\text{eq}})$. We note that in the interpretation of Eq. (2) as a cluster expansion, this means that one assumes the clusters to have their own equilibrium volume irrespective of the average volume of the alloy in which they occur. This corresponds to an assumption of *complete local relaxation*. This can be seen to lead to serious underestimates of the critical temperatures. [To calculate the phase diagram, Kikuchi's cluster variation method (CVM) (Ref. 13) was used with the tetrahedron approximation for the mixing entropy.] The other limit is to assume that each cluster takes the *average volume* (AV) of the alloy at the given composition. In this case, no difference is allowed in the relaxation of $A-A$, $A-B$, and $B-B$ bonds. All bond lengths are determined by the average lattice constant of the alloy. This last approximation yields significant overestimates of the critical temperatures. (Here, the free energy determining the phase diagram was minimized as a function of volume and the cluster population variables of the CVM.)

The above strongly suggests that the treatment of the local relaxations is crucial to the scale of the critical temperatures in the phase diagram. Several schemes have been proposed to include the relaxation energies explicitly in the Hamiltonian.^{7-9,14} Linear-response theory shows that elastic relaxations lead to a *renormalization* of the effective interactions. The latter, however, then acquire a quite long range. An alternative approach, taken, e.g., by Lu *et al.*,¹⁵ is to attempt to include the elastic relaxation energies by using a larger set of many-body interaction parameters which are fitted to an appropriately larger database of ordered structures which are explicitly relaxed.

Here, we take a simpler approach. We maintain the tetrahedron approximation but allow the clusters to have an *effective volume*. The idea is that each cluster must be allowed to have its own *local* volume consistent with the internal strain in the system. As found independently by Chen and co-workers¹⁴ for semiconductor alloys, this

leads to an important renormalization of the cluster energies. In their work, the clusters were embedded in an isotropic effective medium with elastic constants appropriate for the alloy. In our model, the effective local volume of each cluster type is determined by the *experimentally* observed (or independently calculated) distribution of average $A-A$, $A-B$, and $B-B$ bond lengths in the alloy as a function of its composition. No adjustable parameters are used. The plausible approximation made in our approach is to replace the irregular tetrahedra consistent with the local bond lengths by regular tetrahedra of the same volume. The CW approach is used to equate the energy per atom of the $A_{4-n}B_n$ tetrahedron with that of the corresponding CW-ordered crystal structure, but now at the *effective volume* $V_n(x)$.

Information about the bond-length distribution is already available for several systems either from experimental data,¹⁶ from semiempirical semiclassical potential simulations for large (~ 4000 atom) unit cells,¹⁷ or from first-principles calculations of the so-called "special quasirandom structures."¹⁸ These various sources lead to a consistent picture of the nearest-neighbor bond-length distributions in alloys with large size mismatch between the atoms. As an example, the bond lengths used in our calculation for Ni-Pt, based on Ref. 17, are sketched in Fig. 1. (We approximately linearized the distance vs concentration curves and made the end-point lattice constants compatible with our calculated values.) Clearly, the individual bond lengths all deviate significantly from Vegard's law and from the ideal bond lengths (d_{AA}^0 , d_{BB}^0 , d_{AB}^0), the two limits considered above. Similar trends have been obtained for other metals both experimentally¹⁶ and theoretically.^{17,18}

As an aside, we note that a simple harmonic nearest-neighbor pair force model with force constants K_{ij} can be used to estimate the relaxation of AB bonds around an A atom and of an AA bond embedded in B in the dilute limit. Fixing the next-nearest-neighbor shell and assuming that $d_{AB}^0 = (d_{AA}^0 + d_{BB}^0)/2$, one obtains

$$d_{AB} - d_{BB}^0 = (d_{AB}^0 - d_{BB}^0)/[1 + 3(K_{BB}/K_{AB})],$$

$$d_{AA} - d_{BB}^0 = (d_{AA}^0 - d_{BB}^0) \frac{2 - (K_{AB}/2K_{AA})}{2 + 3(K_{AB}/K_{AA})}. \quad (3)$$

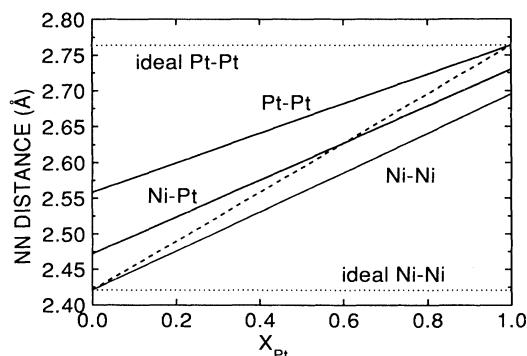


FIG. 1. Nearest-neighbor distances in $\text{Ni}_{1-x}\text{Pt}_x$ alloys as a function of x (solid lines), based on results of Ref. 17, Vegard's law for the average bond length (dashed line), and ideal bond lengths (dotted lines).

TABLE I. Order-disorder critical temperatures (in K).

Approximation ^a	Ni ₃ Pt	NiPt	NiPt ₃
VI	315 (440) ^b	320 (250)	330 (370)
AV	1490 (1840)	1470 (1420)	1410 (1490)
EV	915 (1190)	830 (840)	820 (930)
Ideal c/a	1080	700	970
Expt.	830	940	790

^aVI, volume independent; AV, average volume; EV, effective volume; ideal c/a , uses EV approach; all other cases used experimental c/a ; expt., Ref. 5.

^bNumber in parentheses ASA, other FP.

This extremely simple model already predicts relaxations in reasonable agreement with the more complete calculation of Ref. 17 used here.

Given the individual bond lengths, it is straightforward to calculate the volume $V_n(x)$ of the tetrahedron $A_{4-n}B_n$. The fact that the configurational average $\langle V(x) \rangle = \sum_n P_n V_n(x)$ is close to the Vegard's-law average indicates that the model is internally consistent.

Our calculations of $\Delta E_n(V)$ used density-functional theory in the local-density approximation (LDA) (Ref. 2) with the Hedin-Lundqvist¹⁹ parametrization of exchange correlation.²⁰ We used the linear-muffin-tin-orbital (LMTO) method²¹ to solve the scalar-relativistic non-spin-polarized Kohn-Sham equations self-consistently, using both the atomic sphere approximation (ASA) (including combined correction) and the full-potential (FP) version of the method developed by Methfessel.^{22,23}

The $\Delta E_n(V)$ curves shown in Fig. 2 were obtained using the cohesive energies at the equilibrium lattice constant of each compound calculated with the FP-LMTO method and the equation of state of Rose *et al.*²⁴ using values of the lattice constant a , bulk modulus B , and its pressure derivative B' linearly interpolated between the calculated values for Ni and Pt. The resultant a , B , and B' proved to be in good agreement with our previously calculated ASA values²⁵ for Ni, Pt, and the three compounds. It turns out that the FP values for the energies of formation at equilibrium (-6.3 , -8.7 , and -6.4 mRy for Ni_3Pt , NiPt , and NiPt_3 , respectively) are fairly close to the ASA results (-7.2 , -8.5 , and -6.7 mRy for the CW structures.²⁶

The strain reduction, or renormalization effect, due to the use of the *effective volume* (EV) can be seen explicitly in Fig. 2. For example, for the alloy at a given concentration $x = 0.5$, the energies associated with the various clusters are indicated by the circles for the unrenormalized AV approach $\Delta E_n[V(x)]$ and by the squares in the renormalized EV approach $\Delta E_n[V_n(x)]$.

The phase diagram calculated using the renormalized (FP-LMTO) tetrahedron energies is shown in Fig. 3, along with the experimental phase diagram. Table I sum-

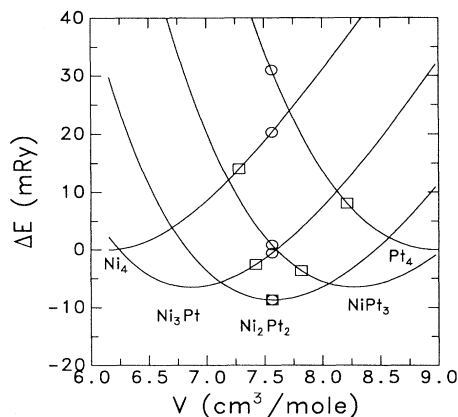


FIG. 2. Formation energies $\Delta E_n(V)$ (solid lines) for the Ni-Pt system. The circles and squares indicate the energies used at $x = 0.5$ in the CW approach without and with the effective volume renormalization, respectively.

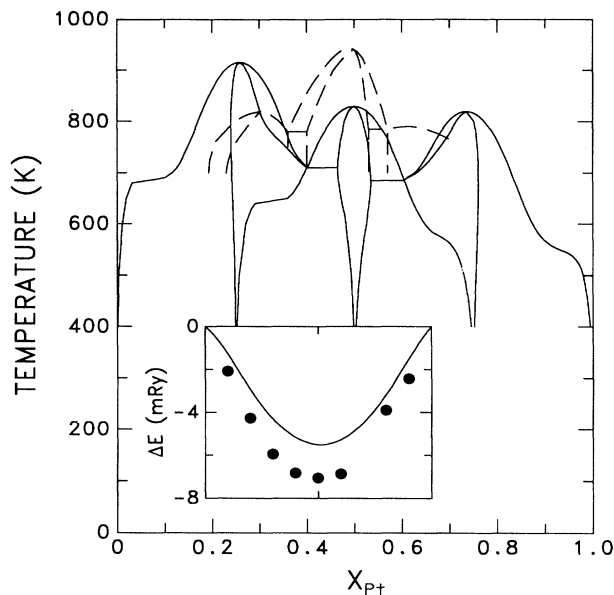


FIG. 3. Experimental (dashed line) and calculated (solid line) phase diagram for the Ni-Pt system using the effective volume approach and FP-LMTO energies of formation. The inset shows the experimental (\bullet) and calculated (solid line) formation energy at 1473 K.

marizes the critical temperatures obtained in the various treatments. The first observation is that the scale of the order-disorder critical temperatures is in good agreement with the experimental values, the maximum deviation being ~ 100 K. The experimental uncertainties are probably of order 50 K. One can see from Table I that both for ASA and FP the major improvement over the conventional CW approaches in the order-disorder temperatures derives from the use of the effective volume approach. We also observe a significant improvement in the ordering of the critical temperatures, in particular, a lowering of $T_c(\text{Ni}_3\text{Pt})$ with respect to $T_c(\text{NiPt})$ due to the use of the FP as opposed to the ASA. Also, we note that using the experimental instead of the ideal c/a ratio for the L_{10} structure has a similar effect. A small residual error in the energies of formation (conceivably due to the LDA) or the absence of explicit long-range interactions may be responsible for the remaining discrepancy.

The inset of Fig. 3 shows that the formation energy of the disordered fcc phase at 1473 K obtained from the calculated CVM cluster population is in good agreement with the experimental data.²⁷ The fact that the same approach provides good agreement with thermodynamic data on enthalpies of formation and with critical temperatures of the phase diagram indicates that the present approach contains the essential physics.

In summary, we have shown that the energetics and the temperature composition phase diagram of a binary alloy with considerable size mismatch can be described fairly well by the nearest-neighbor tetrahedron effective interactions provided the latter are obtained from clusters with the appropriate *effective volume*. The latter must be consistent with the bond-length distribution in the system known either from experiment or from explicit

treatments of the elastic relaxations. It is important to point out that the effective volume $V_n(x)$ depends on the alloy composition and thus our resulting Ising parameters also obtain an explicit concentration dependence. In our approach, the cluster energies are derived by the CW method, but, clearly, this is not an essential requirement. One might conceivably also obtain the cluster energies for a cluster embedded in some effective medium. The essential point is that the cluster must have the appropriate volume. Although the importance of strain effects in this alloy system could have been anticipated, the quantitative success of our approach in determining the energy scale of the phase diagram may come somewhat as a surprise in view of the uncertainties associated with the truncation of the CW cluster expansion. We believe it indicates that the temperature scale of the alloy is mainly

set by the nearest-neighbor interactions when these are determined from a realistic model. Nevertheless, explicit inclusion of long-range interactions may be important to obtain the correct ordering of the critical temperatures. Also, these are obviously necessary to distinguish phases which would be degenerate within the tetrahedron approximation.

This work was partially supported by the NASA Lewis Research Center at CWRU, by Grant No. IN-102392 of the Direccion General de Asuntos de Personal Académico at the UNAM, and Contract No. N00014-89-K-0132 of the Office of Naval Research at SRI. Computational services from the Ohio Supercomputer Center and the Direccion General de Servicios de Cómputo Académico at the UNAM are gratefully acknowledged.

*Present address.

- ¹J. W. D. Connolly and A. R. Williams, *Phys. Rev. B* **27**, 5169 (1983).
- ²P. Hohenberg and W. Kohn, *Phys. Rev.* **136**, B864 (1964); W. Kohn and L. J. Sham, *ibid.* **140**, A1133 (1965).
- ³M. Sluiter and P. E. A. Turchi, *Phys. Rev. B* **40**, 11215 (1989).
- ⁴J. M. Sanchez, F. Ducastelle, and D. Gratias, *Physica A* **128**, 334 (1984).
- ⁵C. E. Dahmani, thesis, Université Louis Pasteur, 1985.
- ⁶C. E. Dahmani, M. C. Cadeville, J. M. Sanchez, and J. L. Morán-López, *Phys. Rev. Lett.* **55**, 1208 (1985).
- ⁷S. Froyen and C. Herring, *J. Appl. Phys.* **52**, 7165 (1981).
- ⁸S. Marais, V. Heine, C. Nex, and E. Salje, *Phys. Rev. Lett.* **66**, 2480 (1991).
- ⁹S. de Gironcoli, P. Giannozzi, and S. Baroni, *Phys. Rev. Lett.* **66**, 2116 (1991).
- ¹⁰G. Treglia and F. Ducastelle, *J. Phys. F* **17**, 1935 (1987).
- ¹¹Z. W. Lu, S.-H. Wei, and A. Zunger, *Phys. Rev. Lett.* **68**, 1961 (1992); **66**, 1753 (1991).
- ¹²F. J. Pinski, B. Ginatempo, D. D. Johnson, J. B. Staunton, G. M. Stocks, and B. L. Györfy, *Phys. Rev. Lett.* **66** 766 (1991); **68**, 1962 (1992).
- ¹³R. Kikuchi, *Phys. Rev.* **81**, 988 (1951); *J. Chem Phys.* **60**, 1071 (1974).
- ¹⁴A.-B. Chen and A. Sher, *Phys. Rev. B* **32**, 3695 (1985); A. Sher, M. van Schilfgaarde, A.-B. Chen, and W. Chen, *ibid.* **36**, 4279 (1987); A.-B. Chen, A. Sher, and M. Berding, *ibid.* **37**, 6285 (1988).
- ¹⁵Z. W. Lu, S.-H. Wei, A. Zunger, S. Frota-Pessoa, and L. G. Ferreira, *Phys. Rev. B* **44**, 512 (1991).
- ¹⁶G. Renaud, N. Motta, F. Lançon, and M. Belakhovsky, *Phys. Rev. B* **38**, 5944 (1988).
- ¹⁷N. Mousseau and M. F. Thorpe, *Phys. Rev. B* **45**, 2015 (1992).
- ¹⁸Z. W. Lu, S.-H. Wei, and A. Zunger, *Phys. Rev. B* **44**, 3387 (1991).
- ¹⁹L. Hedin and B. I. Lundqvist, *J. Phys. C* **4**, 2064 (1971).
- ²⁰Changes ≤ 0.5 mRy were found using the exchange correlation of D. M. Ceperley and B. Alder, *Phys. Rev. Lett.* **45**, 566 (1980); J. P. Perdew and A. Zunger, *Phys. Rev. B* **23**, 5048 (1981).
- ²¹For a recent account, see O. K. Andersen, A. V. Postnikov, and S. Yu Savrasov, in *Applications of Multiple Scattering Theory to Materials Science*, edited by W. H. Butler, P. H. Dederichs, A. Gonis, and R. L. Weaver, *Mater. Res. Soc. Symp. Proc. No. 253* (Materials Research Society, Pittsburgh, 1992), p. 37.
- ²²M. Methfessel, *Phys. Rev. B* **38**, 1537 (1988).
- ²³Two-panel calculations were used to include the Ni $3p$, $3s$ and Pt $5p$, $5s$ band dispersion and their coupling to the valence d -states. The muffin-tin radii were chosen to be almost touching with a fixed ratio of $R_{Ni}/R_{Pt} = 0.94$ and to scale with the lattice constant so as to maintain a constant and maximal sphere-volume-filling fraction. A well converged "triple- κ " basis set with angular momentum cut-offs fdp was used. Brillouin-zone integrations were carried out using the tetrahedron method with 120 k points in the irreducible wedge. Tests showed that the global uncertainty of the results from various parameter choices was less than 0.5 mRy/atom.
- ²⁴J. H. Rose, J. R. Smith, F. Guinea, and J. Ferrante, *Phys. Rev. B* **29**, 2963 (1984).
- ²⁵C. Amador, W. R. L. Lambrecht, and B. Segall, in *Applications of Multiple Scattering Theory to Materials Science*, edited by W. H. Butler, A. Gonis, P. H. Dederichs, and R. L. Weaver, *Mater. Res. Symp. Proc. No. 253* (Materials Research Society, Pittsburgh, 1992), p. 297.
- ²⁶For some less symmetric structures, such as $Z2$ (Ref. 15), the FP results deviate significantly from our earlier ASA results (Ref. 25). Details will be published elsewhere. We thank A. Zunger for pointing out this problem.
- ²⁷R. A. Walker and J. B. Darby, *Acta Metall.* **18**, 1261 (1970).